Electronic Supplementary Material (ESI) for Physical Chemistry Chemical Physics.
This journal is © the Owner Societies 2021

The formation and migration of non-equivalent oxygen vacancies in $PrBaCo_{2-x}M_xO_{6-\delta}$, where M = Fe, Co, Ni and Cu

V.P. Zhukov,[1] E.V. Chulkov,[2,3] B.V. Politov,[1] A.Yu. Suntsov,[1]* V.L. Kozhevnikov[1]

[1]Institute of Solid State Chemistry, 620990 Pervomaiskaya str. 91, Ural Branch of RAS, Yekaterinburg, Russia
[2]Donostia International Physics Center and Departamento de Fisica de Materiales, Facultad de Ciencias Quimicas, Universidad del Pas Vasco, Apdo. 1072, 20080 San Sebastian/Donostia, Spain
[3]St. Petersburg State University, 199034 St. Petersburg, Russia

Supplementary materials

S1. Calculation methodology

Among a variety of different implementations, a very popular is the DFT+U approach, which takes into account the U correction for on-site Coulomb interactions and provides a reliable analysis of the properties at a low computational cost. Though attempts are known of *ab initio* calculations[1,2,3] the U correction is introduced empirically most often with the resulting values being dependent on the amount of 3d electrons and which property is fitted.[4,5] As a consequence, the comparison of changes in $PrBaCo_2O_{6-\delta}$ at the substitution of cobalt by different transition metals appears to be inconclusive. In other words, with different U values in cobalt and other 3d metals, we obtain a spread in calculated observables (structural parameters, energies of defect formation, etc.) and the problem of resolving which ones are best. Moreover, interactions of cobalt with other 3d metals in the crystalline lattice vary being depend on the number of electrons in the 3d metal. Taking this difference into account necessitates the introduction of local U parameters thus resulting in significantly complicated computational problems and a sharp increase of the computation cost. Therefore, all calculations are carried out in GGA approximation with PBE exchange correlation potential[6] as implemented in the *ab initio* simulation VASP 5.2 codes.[7] The electron shells are described by pseudo-potentials supplied with the codes. The corresponding valence electron configurations are given in Table S1.

Table S1 Valence electron configurations of different atoms

Element	Pr	Ba	Fe	Co	Ni	Cu	O
Valence electrons	$5s^25p^66s^25d^1$	$5s^25p^66s^2$	$3d^74s^1$	$3d^84s^1$	$3d^94s^1$	$3d^{10}4s^1$	$2s^22p^4$

The contribution from praseodymium 4f states is disregarded following experimental data.[8] The convergence tests with regard to the values of k-vectors and cut-off energy are carried out for the parent supercell $Pr_9Ba_9Co_{17}M_1O_{54}$ with M = Co, shown in Fig. S1.

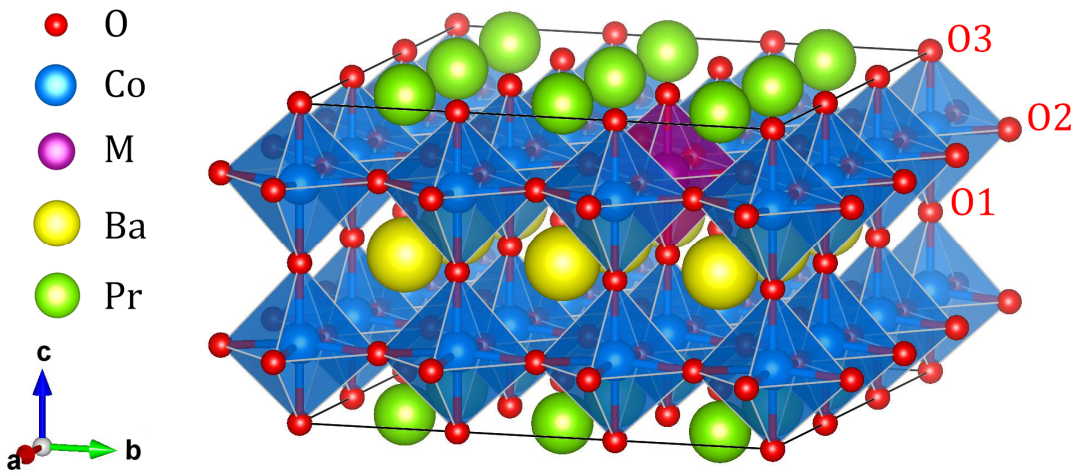

Fig. S1. A sketch of the $Pr_9Ba_9Co_{17}M_1O_{54}$ supercell used in calculations.

It is found that the optimized balance of speed and precision can be attained using 4×4×6 mesh, which corresponds to 18 irreducible k-vectors in the Brillouin zone, and cut-off of 400 eV. Similar methodology is utilized for the supercells containing dopants and oxygen vacancies. The obtained self-consistency of the total energy calculations was no worse than 10^{-5} eV. The structural optimization, i.e. relaxation of atomic positions and lattice constants according to atomic forces, was fulfilled. The minimum of the total energy was considered attained when energy variations at consecutive iteration steps did not exceed 0.005 eV. The spin polarized calculations were carried out assuming ferromagnetic ordering observed below 180 K in $PrBaCo_2O_{6-\delta}$ at $\delta < 0.15$.[9] Notice here that a number of magnetic states are known to exist in the layered cobaltites. For instance, $PrBaCo_2O_5$ is antiferromagnetic at room temperature.[10] The increase of oxygen content is accompanied by the transition from paramagnetic to ferromagnetic state in $PrBaCo_2O_{5.4}$ at 260 K, which is replaced by the mixture of ferromagnetic and antiferromagnetic phases at 200 K, while further decrease of temperature results in entirely antiferromagnetic ordering at 100 K.[11] These observations suggest that phonon and elastic energy may contribute to stabilization of different magnetic configurations. However, these contributions are believed to be small compared to the vacancy formation and doping induced local deformation energies. Therefore, calculations at $\delta = 1.11$ were also performed under supposition of ferromagnetic ordering.

The isomorphous capacity of $PrBaCo_2O_{6-\delta}$ at the substitution of cobalt by other cations has been studied in many works. In this relation, it is interesting to examine from first principles the driving factors that may influence the doping process. It can be done considering the introduction of dopants M as a substitution reaction

$$Pr_9Ba_9Co_{18}O_{54-9\delta} + MO \rightleftarrows Pr_9Ba_9Co_{17}MO_{54-9\delta} + CoO \qquad (S1)$$

which is governed by the change ΔG_D of Gibbs free energy

$$\Delta G_D = E_{tot}(M,\delta) - E_{tot}(Co,\delta) + \varepsilon^{\circ}_{CoO} - \varepsilon^{\circ}_{MO} - T\left(\Delta S^{\circ} + \int_0^T \frac{1}{T^2}\left[\int_0^T \Delta C_p dT\right] dT\right) \qquad (S2)$$

where $E_{tot}(Co,\delta)$ and $E_{tot}(M,\delta)$ denote calculated full energy of pristine and doped cobaltites at a given δ value, and respective entropy contributions are neglected because of the small differences in the composition of $PrBaCo_{2-x}M_xO_{6-\delta}$ phases. Parameters $\varepsilon^{\circ}_{CoO}$ and ε°_{MO} stand for similarly calculated values of full energy per formula unit of CoO and MO at zero temperature. The values of ΔS° and ΔC_p, which correspond to the entropy and heat capacity difference of CoO and MO, can be calculated from thermodynamic data.[12,13] Similarly, the assessment of relative stability of V_{O2} and V_{O3} vacancies can be based on DFT computed total energies of supercells with oxygen atoms removed from their respective sites. Notice here that different arrangements of vacancies and dopant atoms are possible. In this work, we consider the limits of the closest and the most distant positions of oxygen vacancies relative to the dopant cation M, Fig. S2.

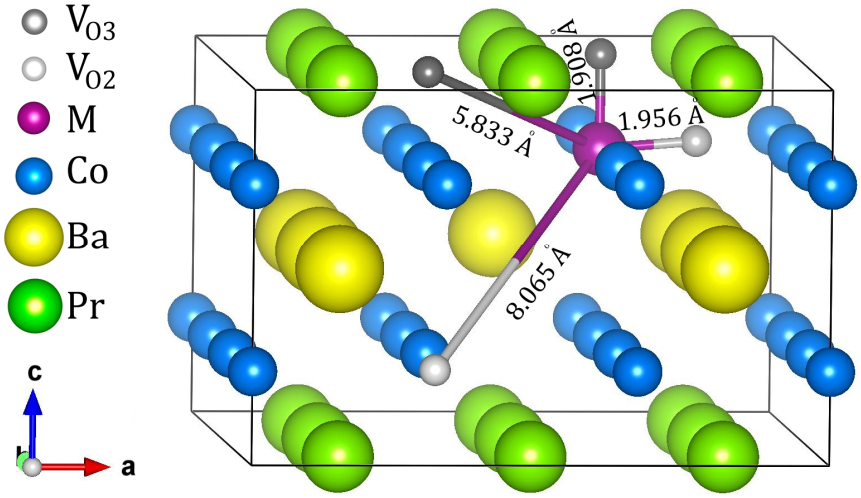

Fig. S2. A sketch of the 3×3×1 supercell showing minimal and maximal possible distances between dopant and oxygen vacancy. Oxygen and interfering Ba/Co atoms are not shown for clarity.

When computing defect energies, one can neglect the changes related to entropy that may vary only slightly with doping, temperature, and oxygen pressure. Notice additionally that the phonon contribution to the enthalpy of vacancy formation is expected to be rather small compared to the electron energy part. Indeed, the standard entropy values for transition metal oxides vary within 2 – 8 kJ·mol^{-1}·K^{-1}, which gives the estimate 0.02 – 0.08 eV/atom for the characteristic phonon enthalpy at 1000 K in reasonable coincidence with the classical limit $3/2k_B \cdot 1000$ K = 0.12 eV/atom. Hence, we conclude that the phonon contribution ca. 0.1 eV or even smaller can be safely neglected. With these assumptions, the change of standard enthalpy $\Delta H^{\circ}_{(\mathrm{M},j|n,m|k)}$ associated with the formation of n vacancies V_{O2} and m vacancies V_{O3} in $PrBaCo_{2-x}M_xO_{6-\delta}$ can be represented as

$$\Delta H^{\circ}_{(\mathrm{M},j|n,k|m)} = \frac{E_{\mathrm{tot}}\left(\mathrm{M}, j+n, k+m\right) - E_{\mathrm{tot}}\left(\mathrm{M}, j, k\right)}{n+m} + \frac{1}{2}\left[\varepsilon^{\circ}_{\mathrm{O}_2} + \int_0^T C_p dT\right] \qquad \text{(S3)}$$

where $E_{\mathrm{tot}}\left(\mathrm{M}, j+n, k+m\right)$ and $E_{\mathrm{tot}}\left(\mathrm{M}, j, k\right)$ are the total energies of the supercells with dopant M, symbols j and k designate the amount of V_{O2} and V_{O3} vacancies before the loss of oxygen, respectively, $\varepsilon^{\circ}_{\mathrm{O}_2} = -10.72$ eV can be taken from[14], and temperature dependence of heat capacity of gas phase oxygen $C_p = f(T)$ is given in JANAF tables.[12] Notice that the disregard of phonon contribution and addition of temperature-dependent corrections just slightly affect the eventually obtained thermodynamic quantities, which are mostly defined by the *ab initio* calculated total energies.

The energy barriers for oxygen migration were calculated using the NEB method supplied with the VASP program package.[15] Seven positions of an oxygen atom were considered along the trajectory of the jump over O2 and O3 positions in $PrBaCo_{1.89}M_{0.11}O_{5.89}$[16] for self-consistent calculations of energy at each position. The calculations were carried out with taking structural relaxation into account. The resulting energy profiles were used to find the activation energy for ion transport.

S2. Charge density maps in $PrBaCo_{2-x}M_xO_6$

Changes in charge distribution at the introduction of dopants in $PrBaCo_2O_6$ are depicted in Figure S3. The ordinate axis shows the entire range of electron charge density values obtained in the calculation.

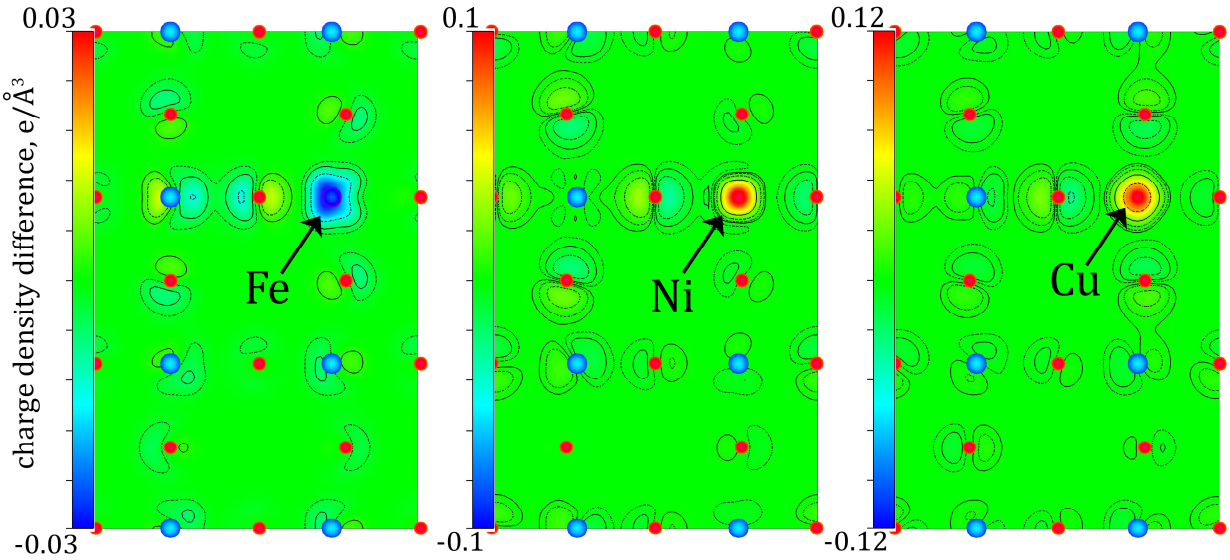

Fig. S3. The calculated difference of charge density distribution in (300) plane of $Pr_9Ba_9Co_{17}M_1O_{54}$ supercell relative to $Pr_9Ba_9Co_{18}O_{54}$. The dopant positions are shown by black arrows. The crystallographic positions of the cobalt and oxygen atoms are shown by blue and red circles, respectively.

S3. Oxygen non-stoichiometry in $PrBaCo_{2-x}M_xO_{6-\delta}$

It is convenient to consider defect formation reactions in the $PrBaCo_2O_{6-\delta}$ based solid solutions by making use of the model proposed in the work.[17] In the present study, the main interest is associated with the redistribution of oxygen vacancies over nonequivalent positions in the region near $\delta = 1$. So large a concentration of oxygen vacancies is accompanied by the exhaustion of mobile *n*-type electronic charge carriers. Therefore, reactions of oxygen positional exchange and depletion can be approximated in Kröger–Vink notation as

$$O_{O2}^{\times} + V_{O3}^{\bullet\bullet} \rightleftarrows O_{O3}^{\times} + V_{O2}^{\bullet\bullet} \quad \text{(S4)}$$

$$O_{O2}^{\times} \rightleftarrows V_{O2}^{\bullet\bullet} + 2e^{/} + \frac{1}{2}O_2 \quad \text{(S5)}$$

$$O_{O3}^{\times} \rightleftarrows V_{O3}^{\bullet\bullet} + 2e^{/} + \frac{1}{2}O_2 \quad \text{(S6)}$$

and treated in the ideal solution approximation. In our consideration, we treat electrons as delocalized. Though not quite true from a physical standpoint, it greatly simplifies the representation and at the same time does not affect the mathematical description of the equilibria. The equilibrium constants for (S4) – (S6) can be represented as

$$\begin{aligned} K_{S4} &= \exp\left(\tfrac{\Delta S_1^0}{k_B}\right)\exp\left(\tfrac{-\Delta H_1^0}{k_B T}\right) = \frac{\left[\mathrm{V}_{\mathrm{O2}}^{\bullet\bullet}\right]\left[\mathrm{O}_{\mathrm{O3}}^{\times}\right]}{\left[\mathrm{O}_{\mathrm{O2}}^{\times}\right]\left[\mathrm{V}_{\mathrm{O3}}^{\bullet\bullet}\right]} \\ K_{S5} &= \exp\left(\tfrac{\Delta S_2^0}{k_B}\right)\exp\left(\tfrac{-\Delta H_2^0}{k_B T}\right) = \frac{\left[\mathrm{V}_{\mathrm{O2}}^{\bullet\bullet}\right] n^2}{\left[\mathrm{O}_{\mathrm{O2}}^{\times}\right]}\sqrt{p_{\mathrm{O}_2}} \\ K_{S6} &= \exp\left(\tfrac{\Delta S_3^0}{k_B}\right)\exp\left(\tfrac{-\Delta H_3^0}{k_B T}\right) = \frac{\left[\mathrm{V}_{\mathrm{O3}}^{\bullet\bullet}\right] n^2}{\left[\mathrm{O}_{\mathrm{O3}}^{\times}\right]}\sqrt{p_{\mathrm{O}_2}} \end{aligned} \tag{S7}$$

where ΔS_i^0 and ΔH_i^0 denote changes of the standard entropy and enthalpy in the *i*'th reaction, and *n* is electron concentration. One can see that the values of ΔS_1^0, ΔS_2^0, ΔS_3^0, ΔH_1^0, ΔH_2^0 and ΔH_3^0 are interdependent. Indeed, the subtraction of (S6) from (S5) results in (S4). Taking into account that the entropy change in (S4) is small[17] and setting it approximately to zero, we have

$$\begin{aligned} &\Delta H_1^0 = \Delta H_2^0 - \Delta H_3^0 \\ &\Delta S_1^0 = 0 \\ &\Delta S_2^0 = \Delta S_3^0 = k_B \ln\left(K_0\right) \end{aligned} \tag{S8}$$

where K_0 is a constant. The equilibrium constants must be complemented with the structure conservation requirements

$$\left[\mathrm{V}_{\mathrm{O2}}^{\bullet\bullet}\right] + \left[\mathrm{V}_{\mathrm{O3}}^{\bullet\bullet}\right] = \delta;\ \ \left[\mathrm{O}_{\mathrm{O2}}^{\times}\right] + \left[\mathrm{O}_{\mathrm{O3}}^{\times}\right] = 5 - \delta;\ \ \left[\mathrm{V}_{\mathrm{O3}}^{\bullet\bullet}\right] + \left[\mathrm{O}_{\mathrm{O3}}^{\times}\right] = 1 \tag{S9}$$

Then, we have

$$\left[\mathrm{V}_{\mathrm{O3}}^{\bullet\bullet}\right] = \delta - \left[\mathrm{V}_{\mathrm{O2}}^{\bullet\bullet}\right];\quad \left[\mathrm{O}_{\mathrm{O3}}^{\times}\right] = 1 - \delta - \left[\mathrm{V}_{\mathrm{O2}}^{\bullet\bullet}\right] \tag{S10}$$

The electrical neutrality condition at $\delta \approx 1.0$ can be written as[17]

$$n = 2\left[\mathrm{V}_{\mathrm{O3}}^{\bullet\bullet}\right] + 2\left[\mathrm{V}_{\mathrm{O2}}^{\bullet\bullet}\right] - 1 = 2\delta - 1 \tag{S11}$$

It follows from (S11) that *n* can be approximated by unity when non-stoichiometry is close or exactly equal to $\delta = 1$. In such a case, the substitution of (S10) and (S8) into (S7) results in

$$K_0 \exp\left(\tfrac{-\Delta H_3^0}{k_B T}\right) = \frac{\left(\delta - \left[\mathrm{V}_{\mathrm{O2}}^{\bullet\bullet}\right]\right)\sqrt{p_{\mathrm{O}_2}}}{1 - \delta - \left[\mathrm{V}_{\mathrm{O2}}^{\bullet\bullet}\right]} \tag{S12}$$

which gives

$$\left[\mathrm{V}_{\mathrm{O2}}^{\bullet\bullet}\right]=\frac{\delta\left(\sqrt{p_{\mathrm{O}_2}}+K_0\exp\left(\frac{-\Delta H_3^0}{k_BT}\right)\right)-K_0\exp\left(\frac{-\Delta H_3^0}{k_BT}\right)}{\sqrt{p_{\mathrm{O}_2}}+K_0\exp\left(\frac{-\Delta H_3^0}{k_BT}\right)} \tag{S13}$$

Using (S13) in the expression for the equilibrium constant of reaction (S5)

$$K_0\exp\left(\frac{-\Delta H_2^0}{k_BT}\right)=\frac{\left[\frac{\delta\left(\sqrt{p_{\mathrm{O}_2}}+K_0\exp\left(\frac{-\Delta H_3^0}{k_BT}\right)\right)-K_0\exp\left(\frac{-\Delta H_3^0}{k_BT}\right)}{\sqrt{p_{\mathrm{O}_2}}+K_0\exp\left(\frac{-\Delta H_3^0}{k_BT}\right)}\right]}{\left\{4-\frac{\delta\left(\sqrt{p_{\mathrm{O}_2}}+K_0\exp\left(\frac{-\Delta H_3^0}{k_BT}\right)\right)-K_0\exp\left(\frac{-\Delta H_3^0}{k_BT}\right)}{\sqrt{p_{\mathrm{O}_2}}+K_0\exp\left(\frac{-\Delta H_3^0}{k_BT}\right)}\right\}}\sqrt{p_{\mathrm{O}_2}} \tag{S14}$$

and resolving (S14) with respect to δ, we arrive at

$$\delta=\frac{4K_0\exp\left(\frac{-\Delta H_2^0}{k_BT}\right)\sqrt{p_{\mathrm{O}_2}}+K_0\exp\left(\frac{-\Delta H_3^0}{k_BT}\right)\sqrt{p_{\mathrm{O}_2}}-5K_0\exp\left(\frac{-\Delta H_3^0-\Delta H_2^0}{k_BT}\right)}{p_{\mathrm{O}_2}+K_0\exp\left(\frac{-\Delta H_2^0}{k_BT}\right)\sqrt{p_{\mathrm{O}_2}}+K_0\exp\left(\frac{-\Delta H_3^0}{k_BT}\right)\sqrt{p_{\mathrm{O}_2}}+K_0\exp\left(\frac{-\Delta H_3^0-\Delta H_2^0}{k_BT}\right)} \tag{S15}$$

that can be transformed into Eq. (1) in the main text with $E_2 \equiv \Delta H_2^0$ and $E_3 \equiv \Delta H_3^0$.

References

(1) Mosey, N. J.; Liao, P.; Carter, E. A. Rotationally Invariant Ab Initio Evaluation of Coulomb and Exchange Parameters for DFT+U Calculations. *J Chem Phys* **2008**, *129* (1), 014103. https://doi.org/10.1063/1.2943142.

(2) Solovyev, I. V.; Dederichs, P. H. Ab Initio Calculations OfCoulomb U Parameters for Transition-Metal Impurities. *Phys Rev B* **1994**, *49* (10), 6736–6740. https://doi.org/10.1017/CBO9781107415324.004.

(3) Aryasetiawan, F.; Karlsson, K.; Jepsen, O.; Schönberger, U. Calculations of Hubbard U from First-Principles. *Phys Rev B - Condens Matter Mater Phys* **2006**, *74* (12), 125106. https://doi.org/10.1103/PhysRevB.74.125106.

(4) Loschen, C.; Carrasco, J.; Neyman, K. M.; Illas, F. First-Principles LDA+U and GGA+U Study of Cerium Oxides: Dependence on the Effective U Parameter. *Phys Rev B - Condens Matter Mater Phys* **2007**, *75* (3), 035115. https://doi.org/10.1103/PhysRevB.75.035115.

(5) Wang, L.; Maxisch, T.; Ceder, G. Oxidation Energies of Transition Metal Oxides within

the GGA+U Framework. *Phys Rev B - Condens Matter Mater Phys* **2006**, *73* (19), 195107. https://doi.org/10.1103/PhysRevB.73.195107.

(6) Perdew, J. P.; Burke, K.; Ernzerhof, M. Generalized Gradient Approximation Made Simple. *Phys Rev Lett* **1996**, *77* (18), 3865–3868. https://doi.org/10.1103/PhysRevLett.77.3865.

(7) Kresse, G.; Furthmüller, J. Efficient Iterative Schemes for Ab Initio Total-Energy Calculations Using a Plane-Wave Basis Set. *Phys Rev B - Condens Matter Mater Phys* **1996**, *54* (16), 11169–11186. https://doi.org/10.1103/PhysRevB.54.11169.

(8) Frontera, C.; García-Muñoz, J. L.; Carrillo, A. E.; Aranda, M. A. G.; Margiolaki, I.; Caneiro, A. Spin State of Co^{3+} and Magnetic Transitions in $RBaCo_2O_{5.50}$ (R=Pr,Gd): Dependence on Rare-Earth Size. *Phys Rev B - Condens Matter Mater Phys* **2006**, *74* (5), 1–11. https://doi.org/10.1103/PhysRevB.74.054406.

(9) García-Muñoz, J. L.; Frontera, C.; Llobet, A.; Carrillo, A. E.; Caneiro, A.; Aranda, M. A. G.; Respaud, M.; Ritter, C.; Dooryee, E. Magnetic and Electronic Properties of the Oxygen-Deficient $PrBaCo_2O_{5+\delta}$ ($\delta > 0.50$). *J Magn Magn Mater* **2004**, *272–276* (III), 1762–1763. https://doi.org/10.1016/j.jmmm.2003.12.1375.

(10) Soda, M.; Yasui, Y.; Sato, M.; Kakurai, K. Magnetic and Charge Ordering Transitions of $PrBaCo_2O_5$. *J Phys Soc Japan* **2005**, *74* (6), 1875–1876. https://doi.org/10.1143/JPSJ.74.1875.

(11) Ganorkar, S.; Priolkar, K. R.; Sarode, P. R.; Banerjee, A. Effect of Oxygen Content on Magnetic Properties of Layered Cobaltites $PrBaCo_2O_{5+\delta}$. *J Appl Phys* **2011**, *110* (5), 5439–5445. https://doi.org/10.1063/1.3633521.

(12) Chase, M. W.; Curnutt, J. L.; Prophet, H.; Syverud, A. N.; Walker, L. C. JANAF Thermochemical Tables, 1974 Supplement. *J Phys Chem Ref Data* **1974**, *3* (2), 311–480. https://doi.org/10.1063/1.3253143.

(13) SpringerMaterials. Thermodynamic Properties of Compounds, NbO to S_2O: Datasheet from Landolt-Börnstein - Group IV Physical Chemistry ·Volume 19A4: ``Pure Substances. Part 4 _ Compounds from HgH_g to ZnTe_g'' in SpringerMaterials. https://doi.org/10.1007/10688868_13.

(14) Zhukov, V. P.; Shein, I. R. Ab Initio Thermodynamic Characteristics of the Formation of Oxygen Vacancies, and Boron, Carbon, and Nitrogen Impurity Centers in Anatase. *Phys Solid State* **2018**, *60* (1), 37–48. https://doi.org/10.1134/S1063783418010304.

(15) Kresse, G.; Marsman, M.; Furthmüller, J. Vienna Ab Initio Simulation Package (VASP), The Guide; Computational Materials Physics, Faculty of Physics, Universität Wien : Vienna, Austria. **2014**.

(16) Zhukov, V. P.; Politov, B. V.; Suntsov, A. Y.; Leonidov, I. A.; Shein, I. R.; Kozhevnikov, V. L. Structural Stability, Defects and Competitive Oxygen Migration in $Pr_{1-x}Y_xBaCo_2O_{6-\delta}$. *Solid State Ionics* **2020**, *347*, 115230. https://doi.org/10.1016/j.ssi.2020.115230.

(17) Suntsov, A. Y.; Politov, B. V.; Leonidov, I. A.; Patrakeev, M. V.; Kozhevnikov, V. L. Improved Stability and Defect Structure of Yttrium Doped Cobaltite $PrBaCo_2O_{6-\delta}$. *Solid State Ionics* **2016**, *295*, 90–95. https://doi.org/10.1016/j.ssi.2016.08.003.